Transmission polarized optical microscopy of short-pitch cholesteric liquid crystal shells

Yong Geng, JungHyun Noh, and Jan P.F. Lagerwall

University of Luxembourg, Physics & Materials Science Research Unit
L-1511 Luxembourg, Luxembourg

ABSTRACT

We recently demonstrated that colloidal crystal arrangements of monodisperse droplets or shells of planar-aligned cholesteric liquid crystal exhibit intricate patterns of circularly polarized reflection spots of different colors. The spots appear as a result of photonic cross communication between droplets, hence the patterns reflect the macroscopic arrangement of droplets or shells. Apart from being an interesting optical phenomenon, it offers attractive application opportunities in photonics and beyond, due to the unique characteristics of the patterns. It turns out that the optical quality of shells is much enhanced compared to that of droplets, hence we focus our attention primarily on shells, of varying thickness. Here we analyze and explain the intriguing textures arising when studying planar-aligned short-pitch cholesteric shells in transmission polarizing optical microscopy. In this case, the texture reflects the properties of each individual shell, without any sign of cross communication, yet also this pattern holds some fascinating mysteries. These can only be elucidated by considering all the peculiar optical properties of cholesterics together, as well as the unusual situation given by the spherical shell geometry.

Keywords: Cholesteric liquid crystals, optical rotation, birefringence, spherical shells, helical structures

1. INTRODUCTION

The extraordinary optical properties of short-pitch cholesteric liquid crystals have been known for decades (the spectacular iridescence of cholesterics played a major role in the discovery of liquid crystals,[1] although it took a long time until the origin of the strong colors was understood) and they have been put to use in various devices, many on commercial scale. Cholesterics (abbreviated N*, as they can be considered as chiral (*) nematics) owe these properties to their internal helical structure, where the director **n** (describing the average orientation of the molecules) is modulated sinusoidally along a direction **k** perpendicular to **n**. In case of short-pitch materials, the period p_0 of this modulation is on the order of 300-500 nm. The most famous consequence of this spontaneous chiral molecule arrangement is the selective reflection of circularly polarized light with the same handedness as the cholesteric helix. Circularly polarized light with the opposite handedness is transmitted, but if the handedness is the same and if the wavelength inside the cholesteric is on the order of the helix pitch (within a band of width $p_0\Delta n$, where Δn is the birefringence), the light cannot propagate, but it is reflected according to Bragg's law, $p_0 \sin\theta = m\lambda_{N*}$, where θ is the angle between the incoming light beam and the surface of the cholesteric material, m is an integer ($m = 1$ for normal incidence) and λ_{N*} is the light wavelength within the cholesteric.

Also outside the selective reflection band the cholesteric behaves quite remarkably. It has an exceptionally high optical rotatory power, diverging on approaching the selective reflection band from either side, and the sign of the rotation is opposite for wavelengths greater and smaller, respectively, than p_0, cf. Fig. 1a. Moreover, once p_0 gets smaller than optical wavelengths, the optical anisotropy changes compared to the non-chiral counterpart. Most nematics are optically positive, $\Delta n > 0$, and **n** defines the optic axis, but for short-pitch cholesterics light in the visible range cannot resolve the structure within each turn of the helix. The result is negative birefringence, $\Delta n < 0$, averaging the behavior of the helically modulated director, and the optic axis has rotated by 90°, now being defined by the helix axis **k** rather than by **n**

Further author information: (Send correspondence to J.P.F.L.)
J.P.F.L.: E-mail: Jan.Lagerwall@lcsoftmatter.com, Telephone: +352 4666446219

Emerging Liquid Crystal Technologies XI, edited by Liang-Chy Chien, Dick J. Broer, Hirotsugu Kikuchi, Nelson V. Tabiryan, Proc. of SPIE Vol. 9769, 97690U
 · doi: 10.1117/12.2216132

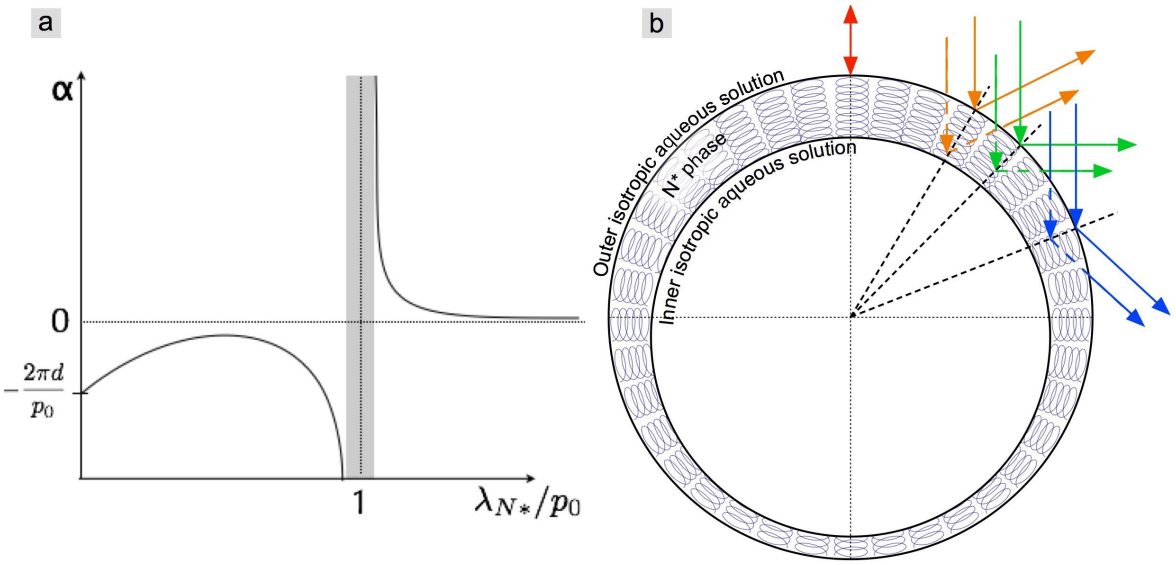

Figure 1. (a) Qualitative sketch of how the polarization direction of linearly polarized light is rotated during transmission through a cholesteric with sample thickness d. This optical rotation α depends strongly on the relation between the light wavelength inside the cholesteric, λ_{N*} and the helix pitch, p_0. The sign of α reverses between different sides of the selective reflection band (indicated with a grey background) around $\lambda_{N*} = p_0$, and it diverges in magnitude upon approaching the selective reflection band from either side. (b) Schematic drawing of the cross section of a planar-aligned short-pitch cholesteric shell, with right-handed helix along the radial direction (illustrated by radial spirals). The shell is thicker at the top than at the bottom due to the slightly greater density of the inner aqueous phase than that of the N* phase. The latter is assumed to reflect in the red regime at normal incidence. A few representative reflection paths are indicated at the top right (in reflection mode, the illumination and observation are assumed to be from the top of the picture).

We recently showed that the selective reflection in combination with the spherical geometry of cholesteric droplets or shells (a thin layer of cholesteric surrounding an internal isotropic liquid droplet, and surrounded by a continuous isotropic phase, cf. Fig. 1b) gives rise to a very interesting new behavior when many such cholesteric spheres are brought close to each other: a photonic cross communication takes place between adjacent spheres, along specific channels defined by Bragg's law and the directions of communication, generating intricate multicolored patterns that can be dynamically tuned by varying the illuminated area.[2,3] Fan et al.[4] and Aβhoff et al.[5] showed that additional dynamics can be added by incorporating a photoresponsive chiral dopant, and by incorporating cholesteric droplets inside an optically isotropic rubber shell, Lee et al. provided high mechanical stability.[6] Following an earlier experiment on lasing from cholesteric droplets,[7] two groups also studied omnidirectional lasing from short-pitch cholesteric shells.[8,9]

With the striking reflective properties of this new configuration for studying and applying cholesteric liquid crystals, the attention has so far been focused on the textures and other signatures of cholesteric spheres in reflection only. However, also the transmission microscopy textures of cholesteric shells are highly intriguing and far from trivial to understand, even though in this case it is the behavior of each individual shell that dictates the results, rather than the arrangement of adjacent shells. In this paper we focus on the transmission textures, presenting the first systematic polarizing microscopy study complemented with a qualitative analysis. We show that all four key aspects of the unique optics of short-pitch cholesterics—selective reflection, strong optical rotation, inversion of optical anisotropy, and rotation of the optic axis from **n** to **k**—must be taken into account to explain all salient features.

2. EXPERIMENTAL

The shells were produced in a capillary microfluidic set-up, fundamentally following the principle developed by Utada et al.,[10] with the details applying to our case described by Noh et al.[11] We use the same cholesteric

liquid crystal mixtures as in our original study,[2] based on the commercial nematic mixture RO-TN 615 (Roche, Switzerland) and the commonly employed chiral dopant CB-15 (Synthon Chemicals, Germany), but to make shells rather than droplets, we here incorporate the same aqueous isotropic phase inside the cholesteric as outside. This phase is a mixture of glycerol (Sigma-Aldrich) and water in an 80/20 volume ratio, to which polyvinylalcohol (PVA, Sigma-Aldrich, $m_w \approx 85,000-124,000$ g mol^{-1}, 99% hydrolysed) was added to stabilize the shells without interfering with the planar alignment promoted by water and glycerol.[11] Because its density is slightly higher than that of the N* mixture, the shell is slightly asymmetric, with thicker top and thinner bottom, as illustrated in Fig. 1b. As reference, a set of homeotropic-aligned non-chiral nematic shells were produced using 4-cyano-4'-*n*-pentylbiphenyl (5CB) as liquid crystal and sodium dodecyl sulfate (SDS) as stabilizer, the latter inducing homeotropic alignment at sufficiently high concentration.[11]

The flow of all fluids was regulated by a four-channel pneumatic microfluidic control unit (Fluigent MFCS-EZ) and the set-up was mounted on a hot stage to ensure a shell production temperature of about 45°C, where the cholesteric mixture is in its isotropic state. Optical characterization was carried out using an Olympus BX51 polarizing optical microscope, in reflection and transmission mode, and pictures were taken using an Olympus DP73 camera mounted on the microscope. Monochromatic illumination was ensured by inserting appropriate interference filters in the illumination light train.

3. RESULTS AND DISCUSSION

An overview of the characteristic textures of cholesteric shells in reflection and transmission, respectively, is provided in Fig. 2. The top row shows the reflection texture of a shell surrounded by many identical shells, without analyzer, between crossed polarizers, and analyzed for left- and right-handed circular polarization, respectively. Here we briefly summarize the key features, because an awareness of the reflection behavior is important also for analyzing the transmission textures, referring the reader to our previous paper[2] for the details. The liquid crystal mixture is tuned for reflecting red light (vacuum wavelength $\lambda_0 \approx 700$ nm) along the helix axis, giving rise to a red reflection spot at the center of the shell, see the red double-headed arrow in the schematic drawing in Fig. 1b. This spot is almost blocked out in Fig. 2c, in which a $\lambda/4$ phase plate is inserted in the microscope such that right-handed circular polarization is absorbed, demonstrating that the cholesteric helix is right-handed. The weak remaining presence of the spot is due to the fact that the phase plate is optimized for green-yellow light ($\lambda_p = 550$ nm), thus it is only approximately fulfilling its function for the $\lambda_0 \approx 700$ nm red light.

Further out towards the perimeter a number of distinct orange and green spots can be clearly detected in panes a, b and d. These are due to the photonic cross communication with the neighbor shells. As illustrated in Fig. 1b green light fulfills the selective reflection condition a certain distance away from the shell center, where the reflected light is directed into the horizontal plane ($700\ \text{nm} \cdot \cos 45^\circ = 495$ nm). This then hits the adjacent shells, which reflect the light back up to the vertical direction, such that the observer sees it. The spots we see in the central shell thus arise from light originally incident on the surrounding shells, which reflect it onto the central shell in the horizontal plane, which then reflects the light back up to us.

A second set of peripheral reflection spots is seen slightly further inside, this time with an orange color. In this case the light incident on the adjacent shells are reflected slightly higher up on each shell (orange reflection path in Fig. 1b), giving it a reflection angle such that it hits the interface between the aqueous continuous phase and the air exactly mid-point between the neighbor and the central shell, where it is reflected back down via a Total Internal Reflection (TIR) event, in such a way that the central shell can reflect also this light back up into the vertical direction, making it visible for the observer.

Fig. 1b illustrates that also other colors, for instance blue light, are reflected by a shell, but in this case the light path does not allow inter-shell communication and the light will not be reflected back up to the observer, hence it is not visible in reflection microscopy. However, as we will see below, this reflection event affects the appearance in transmission. Finally, we have also included a few internal reflection paths in Fig. 1b, illustrated for orange, green and blue light. As explained by Fan et al.,[4] light that hits a droplet or a shell with non-negligible thickness at a point where the helix is not in selective reflection orientation for this wavelength, may enter the shell and then meet a helix in the right orientation further inside. This gives rise to a diffuse radial line rather than a spot. Again, we will see that also this affects the texture of the shell observed in transmission.

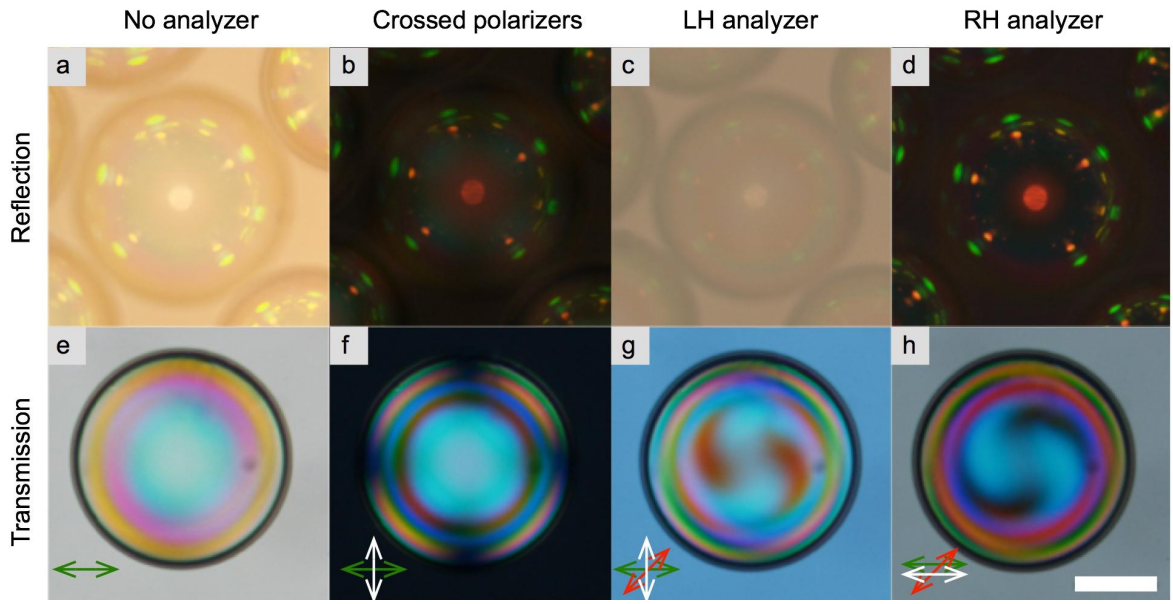

Figure 2. *Top row.* Reflection microscopy textures of a shell of a planar-aligned short-pitch cholesteric (with red selective reflection along the radially oriented helix axis **k**), surrounded by identical shells on all sides. In all cases the illumination is horizontally linearly polarized, in (a) there is no analyzer, in (b) an analyzer is inserted in the crossed orientation, and in (c-d) a $\lambda/4$ plate is inserted, the analyzer being rotated for left- and right-handed circular polarization transmission, respectively. *Bottom row.* Transmission microscopy textures of an isolated shell of the same cholesteric liquid crystal, for the same combinations of polarizer, analyzer and $\lambda/4$ plate (their settings are illustrated along the bottom, applying to both rows). The scale bar is 100 μm.

We can now start analyzing the transmission textures in more detail, starting with the set of four micrographs in the lower row of Fig. 2. In the photo taken without analyzer in pane (e) we see a slight deviation from rotational symmetry around the center. We believe that this quite subtle effect is due to different transmission and reflection coefficients at each shell-aqueous phase boundary, depending on the angle between the incoming polarization and the shell tangent plane at the point of entry. Here we are interested in the internal optics effects related to the cholesteric helix structure, dominating the textures in panes (f) to (h), and we will thus focus on these in the following.

First, we notice in Fig. 2f that we during observation between crossed polarizers can distinguish two distinctly different regimes, in the greater central area and close to the edge, respectively. Around the center a relatively uniform cyan-colored circular area is seen, suggesting that the light is primarily elliptically polarized (including circular polarization as a special case) such that it passes through the linear analyzer to about 50%. For red light within the reflection band passing through the center, along **k**, this is easy to understand: the light is split up into two circular polarized components by the cholesteric helix, the left-handed of which is transmitted.

For the wavelengths surrounding the reflection band, on the other hand, a standard cholesteric does not convert linear-polarized light into elliptically polarized, hence the origin of the cyan-colored elliptically polarized central area is not immediately obvious. To elucidate this, we need to subdivide also the large central area into two subdomains, first restricting ourselves to the very center of the image, where we can consider that the light passes more or less exactly along the helix axis **k**. In this case, for light in the vicinity of, but not within, the reflection band, the helix rotates the polarization direction extremely strongly, as indicated in Fig. 1a, while maintaining the linear polarization. In fact, since the magnitude of the rotation $|\alpha|$ diverges on approaching the reflection band, we can conclude that even a tiny change in the ratio λ_{N*}/p_0 will lead to a substantial change in the amount of polarization rotation. In other words, we are here in a regime where a change in wavelength λ_N* that is far too small to give an appreciable color difference may easily change the rotation on the order of 90 or even 180°. This means that between crossed polarizers, we will always see a bright picture, because there will

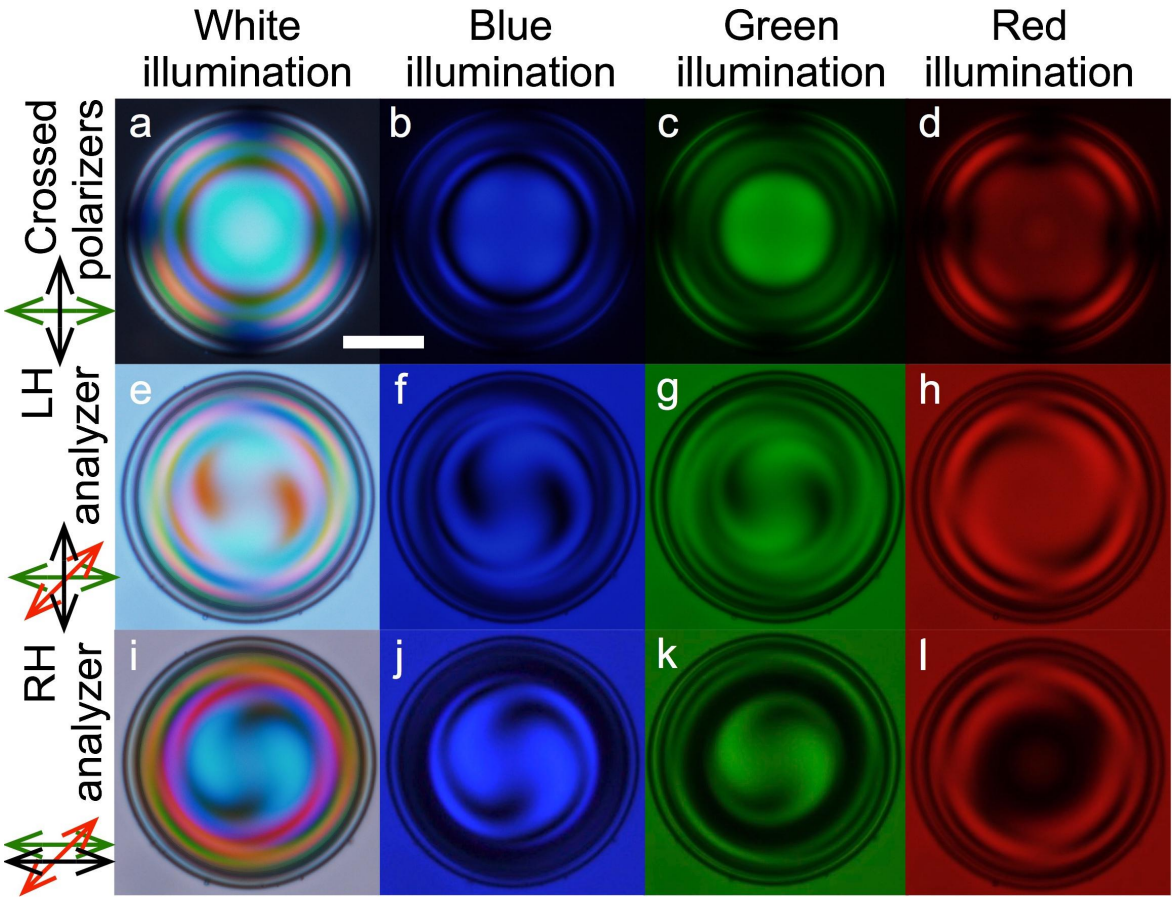

Figure 3. An isolated thin planar-aligned shell of the same liquid crystal as in Fig. 2. The shell is observed in transmission polarized microscopy with white illumination (left column) and with blue, green and red illumination, respectively (columns 2-4). The top row shows the texture between crossed polarizers and rows 2 and 3 shows the textures when a $\lambda/4$ plate is inserted, the analyzer being rotated to the parallel orientation in the bottom row in order to analyze for right-handed circular polarization, while the middle row lets left-handed circular polarization through. The scale bar is 50 μm.

be plenty of wavelengths, all corresponding to more or less the same color, which get through the analyzer. Of course there will be just the same fraction of the incoming light that has been rotated such that it is blocked, and the end result is that, if we integrate over a wavelength regime corresponding to the band width of the color filters we use, we have about 50% of the light going through the analyzer, regardless of how we set it.

Since the light for each wavelength outside the selective reflection band is linearly polarized after passage through the shell it will always go through a circular analyzer to 50%, hence we should see a bright center for linear analyzer as well as for either circular analyzer. This is in fact fundamentally what we see in Fig. 3, where we have added transmission microscopy images for monochrome illumination to make the effects clearer: all panes in the second and third column, showing the shell in blue and green illumination, respectively, for linear, left-handed circular and right-handed circular analyzer, have a rather bright center. The two images for left-handed analyzer are slightly darker at the center, demonstrating that this rough analysis is a bit too simplistic (we must for instance consider the lower value of $|\alpha|$ for blue than for green light), but qualitatively it explains what we see.

Moving out from the very center, we must for this curved geometry also take the effect of birefringence into account, increasing in strength as we move away from the center of the image. This is because $\mathbf{k}$, and thus the optic axis, is no longer in the viewing direction when we leave the center, hence we start seeing its

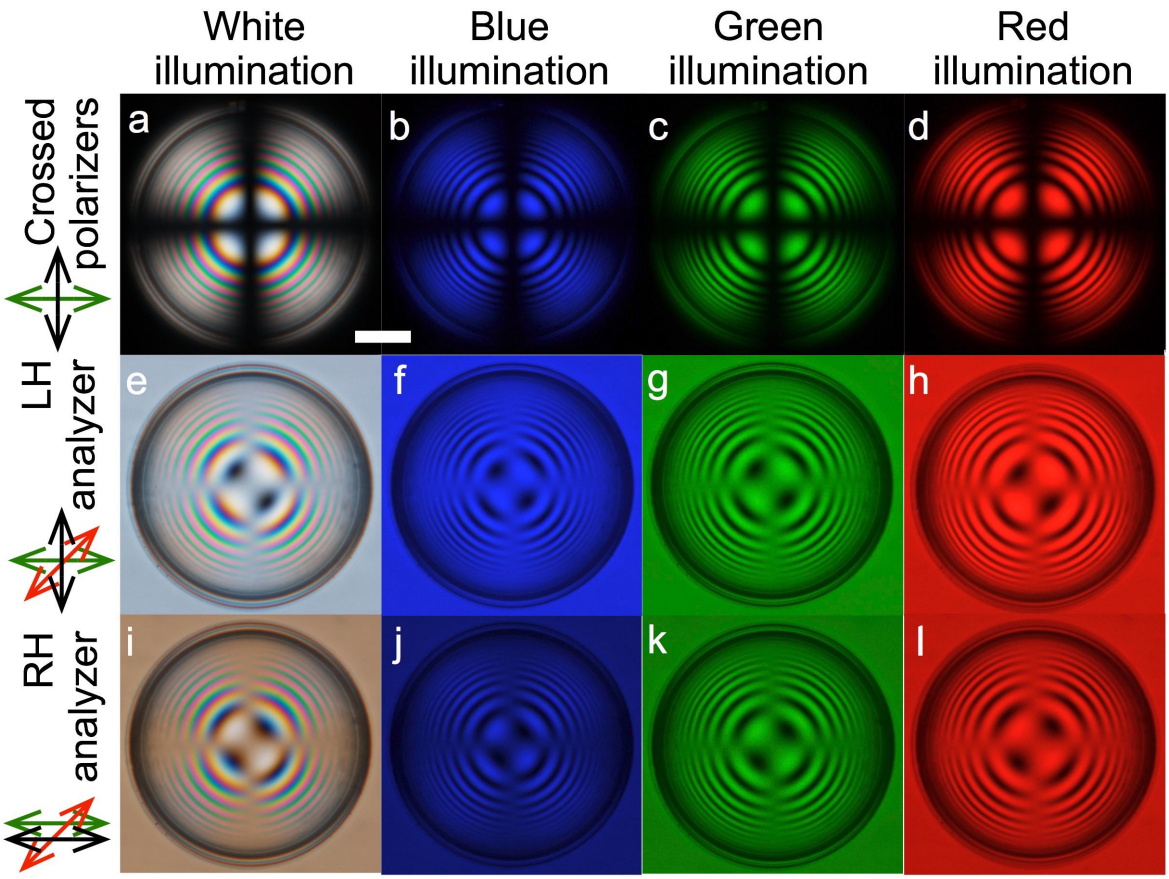

Figure 4. A shell of the non-chiral liquid crystal 5CB, in the nematic state with homeotropic alignment. The arrangement of panes is identical to that in Fig. **??**. The scale bar is 50 μm.

projection in the oscillation plane of the light. To better appreciate this contribution we can compare with the polarizing microscopy transmission textures of a radially aligned nematic shell, e.g. the 5CB shell shown in Fig. 4. The basic crossed-polarizer image when the shell is illuminated by white light (pane a) looks very similar to a conoscopy texture of a flat homeotropic-aligned nematic. As explained by us previously[12] this is because the total birefringence effect is the same in the two cases. The classic conoscopy situation probes all illumination directions through a flat sample, whereas here we probe all possible optic axis directions under vertical illumination.

The shell is decorated by a black cross, reflecting the lack of any birefringence effect from the 5CB shell when the projection of the optic axis is along either the polarizer or the analyzer. For the four quadrants surrounding the cross we have an alternating bright and dark texture along every radius, producing a series of rings that are easier to see when viewing the shell illuminated by monochromatic light, as in the last three columns of the figure. This alternation reflects the radially increasing effective birefringence, the first bright maximum, closest to the center, corresponding to a phase shift $\lambda/2$, the following dark minimum corresponding to a shift of λ, and so on.

By inserting a $\lambda/4$ phase plate in the light path to create an analyzer for circular polarization, as in the lower two rows, the dark cross turns bright, since the light is linearly polarized along the vertical and horizontal directions and thus gets through the circular analyzer. The quadrants are now alternating dark and bright, reflecting the fact that the projection of the optic axis has opposite signs of the angle with respect to the incoming polarization in adjacent quadrants, and we thus get alternatingly right- and left-handed elliptically polarized light. The first maximum in a bright central quadrant, and the first minimum in the adjacent dark

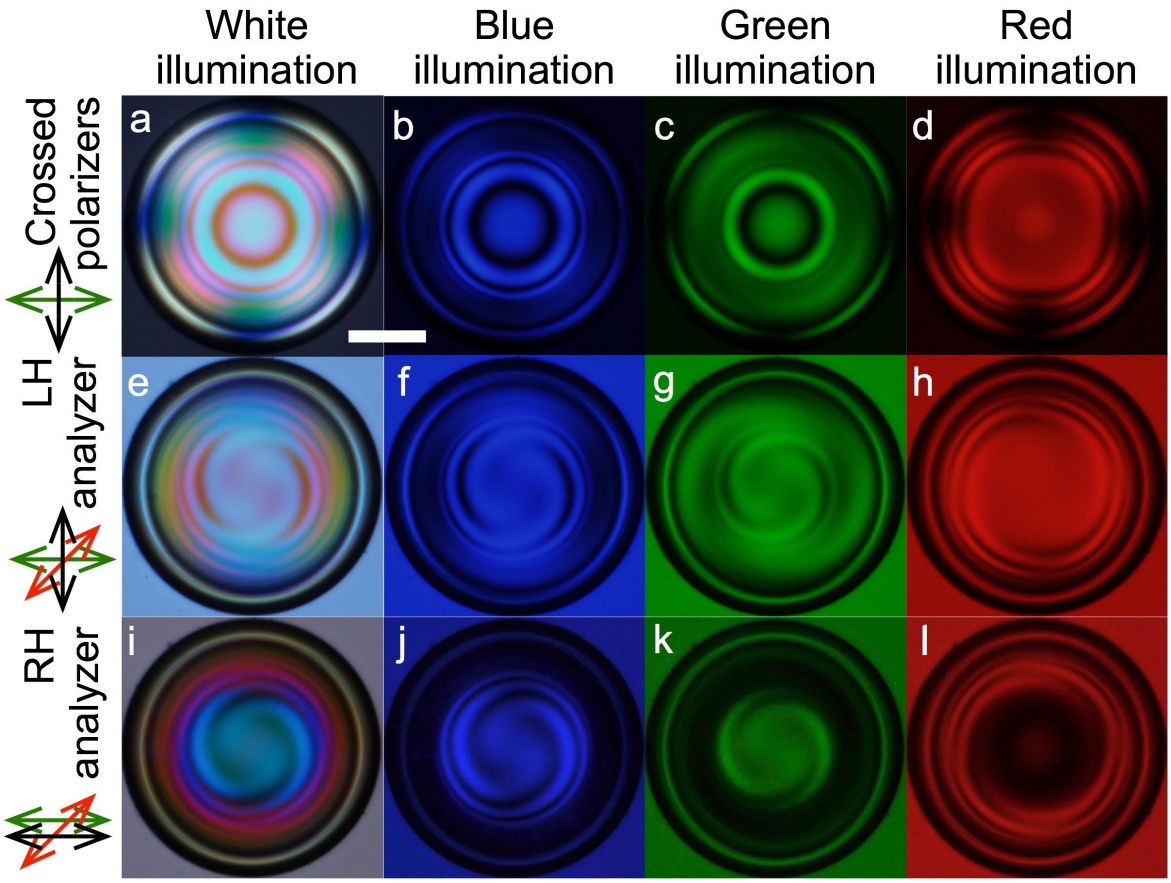

Figure 5. An isolated thick planar-aligned shell of the same liquid crystal as in Fig. 2 and Fig. 3. The arrangement of panes is identical to that in Fig. **??**. The scale bar is 50 μm.

central quadrant, move slightly closer to the center than before inserting the phase plate, as these now correspond to phase shifts of only $\pm\lambda/4$. The ring pattern on moving further away from the center is similar to the case without the phase plate inserted in the microscope, with the important difference that there is an inversion between dark and bright between adjacent quadrants, reflecting the change in handedness. Of course, when we rotate the analyzer by 90°, as in the lowest row, the pattern inverts, as we now analyze with respect to right-handed rather than left-handed circularly polarized light.

We can now go back to explain the textures of the cholesteric shell, adding also monochromatic illumination in Fig. 3. Comparing with the 5CB shell behavior we realize that the reason for the elliptically polarized large area around the center must be birefringence, as the optic axis in the cholesteric shell is defined by $\mathbf{k}$, which is oriented radially, hence leading to an effective birefringence that increases in magnitude as we move away from the image center. An important difference compared to the 5CB case is that Δn here is negative, and the comparison with the non-chiral shell also does not yet explain why there is no cross in the cholesteric shell. We will come back to this slightly more involved issue shortly, but first we move on to explain the appearance towards the perimeter. As in the 5CB case, we here have a set of rings and, at the very perimeter, even dark minima at the top and bottom and on the left and right. In this regime far from the center the inclination of the helix, and thus the optic axis, is now so strong (see Fig. 1b), that birefringence dominates the optical behavior and we get a texture that increasingly looks like that of the 5CB shell in the top row in Fig. 4. The birefringence is much lower (largely due to the helical averaging) than in the 5CB shell, hence there are fewer and thicker rings, but qualitatively the texture is similar away from the center in Fig. 3a-d and Fig. 4a-d.

The cholesteric shell texture gets truly interesting when a $\lambda/4$ phase plate is inserted in the microscope,

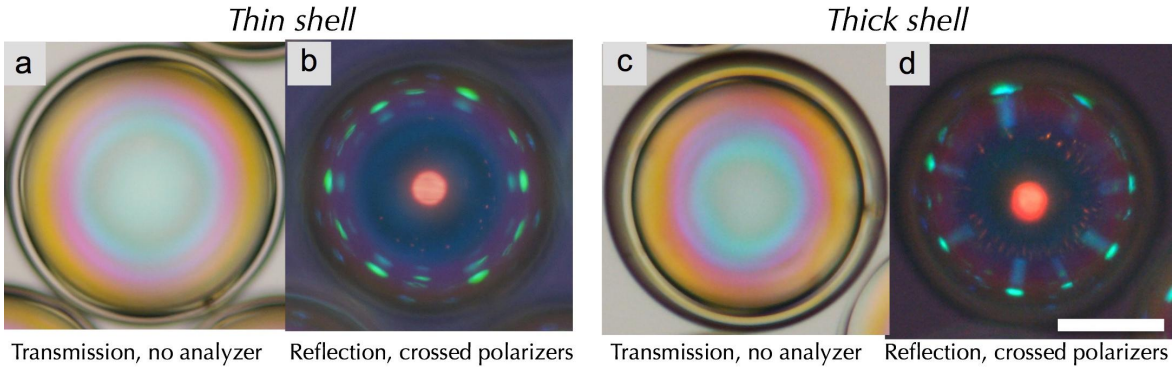

Figure 6. Comparison between a thin and a slightly thicker shell of planar-aligned short-pitch cholesteric liquid crystal (same mixtures as in the previous figures), with transmission without analyzer and in cross-polarized reflection. No orange TIR spots are seen because the sample is kept inside a glass capillary, hence the phase following the outer phase is glass rather than air. The scale bar is 100 μm.

cf. Fig.2g-h and Fig. 3e-l. A 'yin-yang'-like pattern now appears in the central region that was mainly featureless prior to inserting the phase plate, except for the case of red illumination. Moreover, when the analyzer is set to transmit right-handed circular polarization a dark ring appears, covering the central area in case of red illumination (Fig. 3l) and moving outwards as the illumination wavelength gets shorter (Fig. 3k, j). If the shell is made somewhat thicker, as in Fig. 5, the ring in case of green and blue illumination gets thicker.

The dark ring seen with the right-handed circular analyzer setting is rather easy to understand. The cholesteric helix is right-handed, hence it selectively reflects the right-handed circular polarized component within the reflection band entirely. This means that as the light reaches the shell from below, red right-handed polarized light is reflected straight down by the shell around its central area, and only left-handed circular polarized red light is left going through. This explains why the center is dark in Fig. 3l and Fig. 5l. Actually, the transmission wavelength of the red interference filter is apparently slightly smaller than the $\lambda_{N*} = 700$ nm corresponding to normal selective reflection, hence these textures are maximally dark along a ring around the center, where the deviation from 90° in the reflection angle θ means that the reflected wavelength is slightly shorter, as given by Bragg's law, better matching the wavelength of the filter used. The same holds for the rings seen in green and blue illumination. The center is generally bright here, as there is no selective reflection in the blue or green range for light propagating along $\mathbf{k}$, but further out we eventually get to the $\theta = 45°$ condition corresponding to the green cross communication observed in reflection. Since this light is reflected away in case of right-handed circular polarization, the light going through this ring at distances corresponding to such reflection will be (almost) strictly left-handed, thus being blocked by the right-hand analyzer configuration in Fig. 3k and Fig. 5k. For blue light the same situation happens further out towards the shell perimeter, as illustrated in Fig. 1b, and the dark rings in Fig. 3j and Fig. 5j are thus almost at the boundary of each shell.

The reason why the dark rings are wider in Fig. 5j and k than in Fig. 3j and k is that, as mentioned in the beginning, a thick shell allows reflection also from the inside.[4] The internal reflection does not only correspond to a change in vertical reflection location but also in lateral, thus extending the range of green and blue reflections over a range of radii. For green light and observation in reflection this results in a change from spots to diffuse radial lines in the diffraction pattern (an example is shown in Fig. 6). For observation in transmission this simply leads to the dark ring getting increasingly wider, as seen by comparing Fig. 3j-k and Fig. 5j-k.

Let us finally address the most mysterious feature of the cholesteric transmission textures, namely the 'yin-yang' symbol appearing when introducing a $\lambda/4$ phase plate. To understand this we need to consider birefringence, optical rotation and the fact that light passes *twice* through the shell on its way to the observer, once through the bottom half and once through the top half. Comparing first the blue and green textures for circular analyzer of the non-chiral 5CB shell in Fig. 4f-g and j-k with the corresponding textures of cholesteric shells in Fig. 3 and Fig. 5, we note that the bright cross of the non-chiral shell, reflecting the absence of birefringence when light is polarized along or perpendicular to the projection of the optic axis, is absent in the cholesteric

shells. In fact, there is no cross at all here in the central region, but instead we have, in the shell in Fig. 3f and g, mainly bright top and bottom and dark left and right sides for left-handed analyzer, and vice versa for right-handed analyzer. It is thus apparent that the light must be left-handed elliptically polarized towards the top and bottom but right-handed elliptically polarized towards the left and right, which at first appears surprising since one might have expected no birefringence along the vertical and horizontal directions, where the optic axis projection is along or perpendicular to the incoming polarization.

However, we are then forgetting that the passage through the bottom half of the shell introduces optical rotation of the polarization direction due to the helical structure and the vicinity of the reflection band (Fig.1a). This means that when the light reaches the top half of the shell, its polarization direction may have rotated by a certain angle from the original horizontal polarization direction. The magnitude and direction will be identical for a certain distance from the image center, regardless if we go in the vertical or in the horizontal direction, yielding a new polarization direction that we can define by an angle γ away from the vertical direction. Except if γ happens to be a multiple of 90° the light will now experience birefringence when it passes through the *upper* half of the shell, even along the vertical and horizontal directions, because the polarization is no longer parallel or perpendicular to the optic axis projection. Moreover, along the vertical and horizontal directions the optic axis will be rotated from the incoming polarization in opposite directions, meaning that we get right-handed elliptical polarization vertically, and left-handed horizontally, or vice versa.

For light going through the shell in points where the optic axis projection is neither horizontal nor vertical, the birefringence effect is present already during passage through the lower half of the shell, as discussed above in general terms and as seen also in the 5CB shell, but we now realize that this effect is additionally overlaid with the effect of optical rotation. The end result is a complex phase shift that depends both on the distance from the center of the polarizing microscopy image of the shell and the azimuthal angle defining the location around the center. Although we would need to carry out a much deeper analysis, going beyond the scope of this proceedings paper, to reproduce all the details of the pattern, we can now qualitatively understand the origin of the 'yin-yang' pattern, with its opposite elliptical polarizations vertically and horizontally and spiral-like variation that reflects the gradual variations in superposed contributions from birefringence and optical rotation, respectively. The angle γ will of course depend on the thickness of the shell, and this explains why the spiral is narrower, with an alternating dark-bright sequence in the thicker shell in Fig. 5, whereas the spiral in the thinner shell in Fig. 3 is thicker and without the same alternations.

We now finally understand why the whole central area of the shell appears bright between crossed polarizers, over a broad spectrum of colors. Right at the center we have selective transmission (and thus conversion to circular polarization) within the selective reflection band, and extreme rotation of linear polarization direction for other wavelengths. Slightly further away from the center, where the tilt of $\mathbf{k}$ from the propagation direction of the light cannot be neglected, we get elliptical polarization due to the combination of polarization rotation and birefringence.

4. CONCLUSIONS

By systematically studying the transmission polarizing microscopy texture of planar-aligned short-pitch cholesteric shells, under linear as well as circular analyzer conditions and for different monochromatic illumination cases, we can understand the most characteristic features of the peculiar textures. Within a relatively large central area the light is generally elliptically polarized across a broad wavelength spectrum, a result of a combination of selective reflection/transmission at the very center of the shell, combined with rotation of the polarization of incoming linearly polarized light due to the helical director modulation, as well as the birefringence effect that arises when the helix, defining the optic axis in short-pitch cholesterics, has a non-zero projection into the image plane. The fact that the light passes through the light twice means that we must analyze the effect in two steps, finding that the passage through the shell bottom introduces an identical optical rotation when the helix axis is parallel or perpendicular to the original polarization direction, but this leads to a birefringence effect upon passage through the upper shell half, yielding elliptically polarized light with opposite handedness for horizontal and vertical helix orientation, respectively. For intermediate helix orientations optical rotation and birefringence are overlaid during passage through both shell halves. The net effect depends sensitively on distance from the image center as well as inclination with respect to the original polarization direction, eventually producing a 'yin-yang'-like

spiral pattern when the shell is observed with a circular analyzer. Further out towards the shell perimeter, birefringence dominates and we see a ring pattern that reflects the radially varying effective birefringence, due to the rapidly varying helix orientation.

ACKNOWLEDGMENTS

Financial support from the University of Luxembourg (project UNIQUE) and the European Research Council (ERC, Consolidator Project INTERACT, grant number 648763) is gratefully acknowledged.

REFERENCES

[1] Sluckin, T. J., Dunmur, D. A., and Stegemeyer, H., [*Crystals that flow: Classic papers from the history of liquid crystals*], Taylor and Francis, London (2004).

[2] Noh, J., Liang, H.-L., Drevensek-Olenik, I., and Lagerwall, J. P. F., "Tuneable multicoloured patterns from photonic cross communication between cholesteric liquid crystal droplets," *J. Mater. Chem. C* **2**(5), 806–810 (2014).

[3] Noh, J., Drevensek-Olenik, I., Yamamoto, J., and Lagerwall, J. P. F., "Dynamic and complex optical patterns from colloids of cholesteric liquid crystal droplets," *SPIE OPTO, Emerging Liquid Crystal Technologies X* **9384**, 93840T–93840T (2015).

[4] Fan, J., Li, Y., Bisoyi, H., Zola, R., Yang, D., Bunning, T., Weitz, D., and Li, Q., "Light-directing omnidirectional circularly polarized reflection from liquid-crystal droplets.," *Angew. Chem. (Int. Ed.)* **54**(7), 2160–2164 (2015).

[5] Aβhoff, S., Sukas, S., Yamaguchi, T., Hommersom, C., Le Gac, S., and Katsonis, N., "Superstructures of chiral nematic microspheres as all-optical switchable distributors of light.," *Sci. Rep.* **5**, 14183 (2015).

[6] Lee, S., Kim, S., Won, J., Kim, Y., and Kim, S., "Reconfigurable photonic capsules containing cholesteric liquid crystals with planar alignment.," *Angew. Chem. (Int. Ed.)* **54**(50), 15266–15270 (2015).

[7] Humar, M. and Musevic, I., "3D microlasers from self-assembled cholesteric liquid-crystal microdroplets," *Opt. Express* **18**(26), 26995–27003 (2010).

[8] Chen, L., Li, Y., Fan, J., Bisoyi, H. K., Weitz, D. A., and Li, Q., "Photoresponsive monodisperse cholesteric liquid crystalline microshells for tunable omnidirectional lasing enabled by a visible light-driven chiral molecular switch," *Adv. Opt. Mater.* **2**(9), 845–848 (2014).

[9] Uchida, Y., Takanishi, Y., and Yamamoto, J., "Controlled fabrication and photonic structure of cholesteric liquid crystalline shells," *Adv. Mater.* **25**(23), 3234–3237 (2013).

[10] Utada, A., Lorenceau, E., Link, D. R., Kaplan, P. D., Stone, H. A., and Weitz, D. A., "Monodisperse double emulsions generated from a microcapillary device," *Science* **308**(5721), 537–541 (2005).

[11] Noh, J., Reguengo De Sousa, K., and Lagerwall, J. P. F., "Influence of interface stabilisers and surrounding aqueous phases on nematic liquid crystal shells," *Soft Matter* **12**(2), 367–372 (2016).

[12] Liang, H.-L., Enz, E., Scalia, G., and Lagerwall, J., "Liquid crystals in novel geometries prepared by microfluidics and electrospinning," *Mol. Cryst. Liq. Cryst.* **549**, 69–77 (2011).